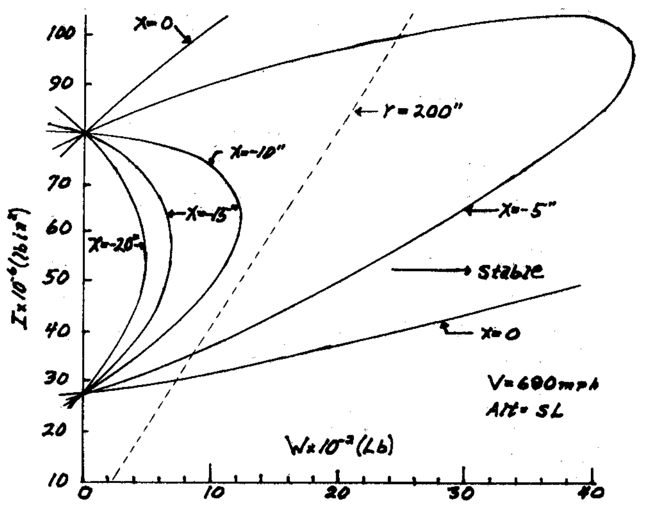

Fig. 1 Variation of critical values of store weight and store inertia, at an assumed airspeed of 680 mph, for several c.g. locations, x.

Hence

$$(\bar{D}_1\bar{E}_2-\bar{D}_2\bar{E}_1)x^2+(\bar{C}_1\bar{E}_2-\bar{C}_2\bar{E}_1)x+(\bar{A}_1\bar{E}_2-\bar{A}_2\bar{E}_1)=0 \qquad (17)$$

$$r^2=-\bar{A}_1+\bar{C}_1x+\bar{D}_1x^2/\bar{E}_1=-\bar{A}_2+\bar{C}_2x+\bar{D}_2x^2/\bar{E}_2 \qquad (18)$$

Numerical Example

Figure 1 shows the results obtained for a typical system[2] with an assumed velocity of 680 mph and consists of plots of store weight W vs store inertia $I = Wr^2$ for five different c.g. locations x. Since the selected velocity in this case lies below the critical flutter speed of the system, the origin of the plot is in the stable region, i.e., in the portion of the plane exterior to all of the contours. Had the assumed velocity been equal to the critical one, the contours would have all passed through the origin, while for velocities above the critical one, the origin would lie interior to all of the curves. As would be anticipated, the region of instability becomes larger as the c.g. location is moved aft.

By assuming a range of velocities, and considering a store with a fixed radius of gyration and c.g. location, the plots of store weight vs store inertia may be converted into a single plot of flutter speed vs store weight. This is accomplished by determining the intersections of the appropriate weight-vs-inertia contour with the straight line; $I = Wr^2$ for the various assumed values of velocity. Coordinates of the desired plot of critical velocity vs store weight are then easily found by cross plotting.

Comparison with Other Methods in Current Use

Some of the more frequently used approaches to the present problem employ the perturbation method[3,4] which shows only the effect of small changes in the store mass and, in addition, usually requires a complete eigenvalue-eigenvector analysis of the flutter matrix, itself a time-consuming process. In contrast, the present method allows one to investigate a wide range of store loadings and unbalances by means of a relatively simple program involving nothing more elaborate than determinant evaluation and the solution of an algebraic equation with real coefficients. The input consists simply of basic mass, stiffness, and aerodynamic data for the wing structure itself, together with a range of velocities and store c.g. locations with output consisting of critical values of store mass and store inertia. Such outputs may be either numerical or graphical if a suitable plot routine is available. Further, the method does not require the use of complicated and specialized electronic analogs as does the approach described in Ref. 1.

In conclusion, it may be added that the method may be adapted to modal-type flutter analyses. In this case the addition of a store results in an augmented matrix of the following form:

$$\begin{bmatrix} A_{i,j}+Mh_ih_j & A_{i,n+j}+Mxh_i\theta_j \\ A_{n+1,j}+Mxh_i\theta_j & A_{n+i,n+j}+M(x^2+r^2)\theta_i\theta_j \end{bmatrix} \qquad (19)$$

where h_i and θ_j are the deflections of the various modes at the station where the mass has been added. By multiplying column 1 by (h_j/h_1), column $(n+1)$ by (θ_j/θ_1) and subtracting, respectively, from columns 2 through n and $(n+2)$ through $2n$, the matrix is brought into the same form as Eq. (4), with the additional terms appearing only in the first and $(n+1)$st column.

References

[1] Epperson, T. B., "F-111A/E ECP0949, ECP10492 Weapon Loadings Flutter Analysis," Rept. FZS-12-305, Aug. 1970, Convair Aerospace Div., General Dynamics Corp., San Diego, Calif.

[2] Bislinghoff, R. A., Ashley, H., and Halfman, R. L., *Aeroelasticity*, Addison-Wesley, Reading, Mass., 1955, pp. 527–631.

[3] Siegel, S. and Andrew, L., "Evaluation of Methods to Predict Flutter of Wings with External Stores," AFFDL-TR-101, May 1970, Air Force Flight Dynamics Lab., Wright-Patterson Air Force Base, Ohio.

[4] Cross, A. K. and Albano, E. A., "Computer Techniques for the Rapid Clearance of Aircraft Carrying External Stores," AFFDL-TR-72-117, Feb. 1973, Pts. I and II, Air Force Flight Dynamics Lab., Wright-Patterson Air Force Base, Ohio.

Integral Approximation for Slender-Body Shock Shapes in Hypersonic Flow

THOMAS D. FIORINO*
Air Force Flight Dynamics Laboratory, Wright-Patterson Air Foce Base, Ohio
AND
MAURICE L. RASMUSSEN†
University of Oklahoma, Norman, Okla.

I. Introduction

THERE have been a number of different methods devised to calculate the shock shapes and flowfields associated with hypersonic flows past slender bodies. Various references germane to the present Note are discussed in Ref. 1. Depending on the objectives desired, the calculation methods soon evolve into lengthy numerical schemes or involved analytical schemes that focus on accuracy and certain specific details, as opposed to consideration of over-all general features of flow problems. In this Note we concern ourselves with a relatively simple method due to Chernyi.[2] By means of integral approximations, Chernyi arrives at a pair of ordinary differential equations that describe the shock shapes and body pressure distribution associated with slender planar bodies and bodies of revolution. In this Note we show that the pair of equations reduces to a single quadrature for the body shape when the shock shape is known. The pressure distribution is determined entirely in terms of the

Received November 15, 1973; revision received July 2, 1974.
Index categories: Shock Waves and Detonations; Supersonic and Hypersonic Flow.

* Capt. U.S. Air Force, Aerospace Engineer. Member AIAA.

† Professor, Department of Aerospace, Mechanical, and Nuclear Engineering. Member AIAA.

shock shape. This solution is simple, analytical, and allows quick calculations to be made that portray the effects of pertinent parameters in a problem. Another exact solution for the shock shape associated with a nongrowing body is also found.

II. Basic Analysis

The derivation of the basic equations starts within the framework of hypersonic small disturbance theory. It is assumed that a very thin layer next to the shock contains all of the mass flow between the shock and the body and that pressure changes between this layer and the body can be neglected. The details of the derivation can be found in Refs. 1 or 2. Let x be the distance measured in the direction of the free-stream, with Mach number, pressure, and ratio of specific heats denoted by M_∞, p_∞, and γ. Further, let $V_s(x)$ be the volume, per unit length, of a cross section of the shock (in the equivalence plane)

$$V_s(x) = 2(1+j)^{-1}\pi^j r_s^{\,1+j} \tag{1}$$

where $r_s(x)$ is the radius of an axisymmetric shock or the half diameter of a two-dimensional shock associated with a symmetric body with planar symmetry aligned with the flow. Here $j = 1$ denotes axisymmetric flow and $j = 0$ denotes planar flow. When the subscript s is changed to b, the above mentioned formulas refer to the body that supports the shock. The corresponding "area" of the shock per unit depth is

$$S(x) = 2(\pi r_s)^j \tag{2}$$

The momentum and energy equations reduce to

$$\gamma p_\infty M_\infty{}^2\, d/dx\,(v_2 V_s) = S(p_b - p_\infty) \tag{3}$$

$$\frac{d}{dx}\left[\frac{2p_b(V_s - V_b)}{\gamma-1} + \gamma p_\infty M_\infty{}^2 V_s v_2{}^2\right] = \frac{2p_\infty}{\gamma-1}\frac{dV_s}{dx} + 2p_b\frac{dV_b}{dx} \tag{4}$$

where the dimensionless velocity v_2 represents the speed of the gas, normalized with the freestream velocity, behind a normal shock propagating into an ambient medium

$$v_2(x) = [2r_s'/(\gamma+1)]\,[1-(1/M_\infty{}^2 r_s'^2)] \tag{5}$$

The pressure on the body surface is denoted by p_b and r_s' is the derivative with respect to x. The pressure can be eliminated between Eqs. (3) and (4) and an equation relating the shock and body radii obtained as follows:

$$\gamma H(dV_b/dx) + V_b(dH/dx) = \gamma G(x) \tag{6}$$

where

$$H(x) \equiv M_\infty{}^{-2} + \gamma S^{-1}(d/dx)(V_s v_2) \tag{7}$$

$$G(x) \equiv \frac{d}{dx}\left[\frac{\gamma-1}{2}V_s v_2{}^2 + \frac{V_s}{\gamma}(H - M_\infty{}^{-2})\right] \tag{8}$$

Integrating for the body shape $V_b(x)$ by means of an integrating factor, we obtain

$$V_b(x) = H^{-1/\gamma}\int_0^x H^{-1+1/\gamma}\,G\,dx + CH^{-1/\gamma} \tag{9}$$

where

$$C \equiv H(O)^{1/\gamma}V_b(O) \tag{10}$$

Equation (9) constitutes the general solution for the inverse problem. In the present theory, both the shock and body vanish at $x = 0$: $V_s(O) = V_b = 0$. For sharp-pointed shocks, $H(O)$ is a finite constant, and the constant of integration C vanishes. For blunt-nosed shocks, r_s' and $H(O)$ are both infinite, and for this case the constant C is indeterminate. This indeterminate constant can be associated with the entropy-displacement thickness. The pressure on the body is determined entirely by the shock shape by means of Eq. (3).

III. Examples

For sharp conical shocks ($j = 1$) and sharp wedge shocks ($j = 0$) described by $r_s = \beta x$, Eq. (9) yields $r_b = \delta x$, where the ratio of shock to body angle is given by

$$\frac{\beta}{\delta} = \left[\frac{\gamma+1}{2} + \frac{1}{M_\infty{}^2\delta^2}\right]^{1/2} \qquad \text{cone} \tag{11}$$

$$\frac{\beta}{\delta} = \frac{\gamma+1}{4} + \left[\left(\frac{\gamma+1}{4}\right)^2 + \frac{1}{M_\infty{}^2\delta^2}\right]^{1/2} \qquad \text{wedge} \tag{12}$$

The surface pressure coefficient determined from Eq. (3) is found to be $C_p = 2\delta^2$ for the cone and

$$\frac{C_p}{\delta^2} = \frac{\gamma+1}{2} + \left[\left(\frac{\gamma+1}{2}\right)^2 + \frac{1}{M_\infty{}^2\delta^2}\right]^{1/2} \tag{13}$$

for the wedge. Expression (11) has also been obtained by another derivation from small disturbance theory[3] and shown to be very accurate for small angles. Equations (12) and (13) are well-known results obtained from hypersonic small disturbance theory.[4,5] As this example demonstrates, the shock and body-shape relationships are accurately predicted, but the pressure for the axisymmetric case is not as accurately determined as that for the planar case. Treatment of ogive shapes and other pointed shapes can be found in Ref. 1.

For power-law blunt nosed shocks described by $r_s = Ax^n$, where $n < 1$, formula (9) yields, for $M_\infty = \infty$

$$r_b^{\,j+1} = Br_s^{\,j+1} + \tilde{C}x^{2(1-n)/\gamma} \tag{14}$$

where

$$B \equiv \frac{[(3-j)n-2+j][\{1+\gamma(3+2j)\}n-\gamma-1]}{(\gamma+1)[(2+j)n-1][(\gamma+2-j)n-2+j]} \tag{15}$$

and $\tilde{C}$ is a new undetermined constant. The value of B given by Eq. (15) compares very well with more sophisticated self-similar theories[1] in which $\tilde{C} = 0$. When $n = 2/(3+j)$, however, the self-similar body vanishes; that is, $B = 0$, and the body is given entirely by the second term in Eq. (14). For this case, Yakura[6] determined by means of matched asymptotic expansions that the body shape grows with x to the same power as predicted by expression (14). Formula (14) also has the same form as a solution obtained by Guiraud et al.[7] Thus the present theory contains within it entropy-displacement effects, associated with the constant $\tilde{C}$ for the inverse problem. A simple means for evaluating $\tilde{C}$ is discussed in Ref. 1.

IV. Direct Solution for Nongrowing Bodies

When V_b is set equal to a constant, Eq. (6) can be integrated once and written

$$2(V_s - V_b)H + \gamma(\gamma-1)V_s v_2{}^2 = \gamma(\gamma+1)C_1 + 2V_s M_\infty{}^{-2} \tag{16}$$

where C_1 is a constant of integration. We now consider the hypersonic limit, $M_\infty \to \infty$, and note that C_1 can be evaluated in terms of the drag coefficient of the body[1]: $C_1 \equiv \varepsilon V_b C_{D_N}$, where $\varepsilon \equiv (\gamma-1)/(\gamma+1)$ and $C_{D_N} \equiv 2D/\gamma p_\infty M_\infty{}^2 V_b$. It is now possible to integrate Eq. (16) twice more and determine the shock shape in terms of the quadrature

$$x = K_1{}^{-1}\int_{V_{s_0}}^{V}\left[V + V_b/2\varepsilon + K_2(V - V_b)^{-2\varepsilon}\right]^{-1/2} V^{1/(1+j)}\,dV \tag{17}$$

where

$$K_1 \equiv (\gamma+1)[\pi^j 2\varepsilon V_b C_{D_N}/(1+2\varepsilon)]^{1/2}$$

and K_2 and V_{s_0} are constants of integration. The pressure on the surface of the body, as determined by Eq. (3), is found to be

$$C_p = \frac{K_1{}^2}{(\gamma+1)\pi^j}\frac{1}{V_s}\left[1 - 2\varepsilon K_2(V_s - V_b)^{-(1+2\varepsilon)}\right] \tag{18}$$

The constant K_2 affects the pressure distribution but does not contribute to the drag.

Because Eq. (17) allows for a body of finite thickness and accounts for entropy-displacement effects, as reflected by the as yet undetermined constants of integration K_2 and V_{s_0}, it is more complicated than its counterpart determined by blast-wave theory. We can simplify the results by assuming that the shock stand-off distance is approximately zero at the nose-body

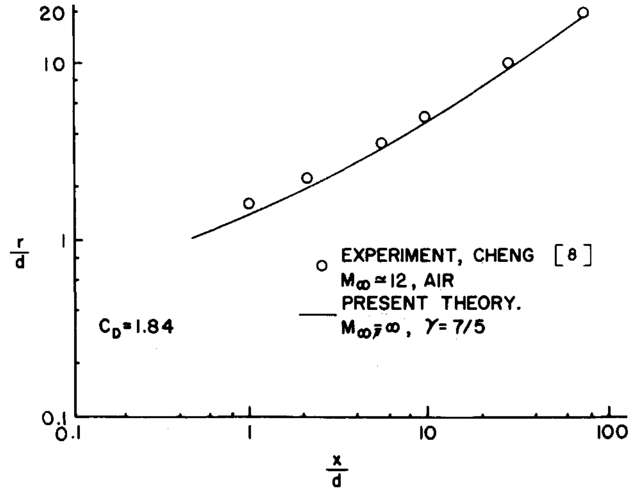

Fig. 1 Shock shape for a flat plate with a flat nose.

junction and set $V_{s_0} = V_b$. In order for C_p now to be finite at $x = 0$, we set $K_2 = 0$, and this also gives a finite slope to the shock at $x = 0$.

The integral in Eq. (19) now can be easily evaluated when $K_2 = 0$, and we obtain for axisymmetric bodies ($j = 1$)

$$x = \frac{\pi r_b^2}{K_1(2\varepsilon)^{1/2}}\left[z(2\varepsilon z^2+1)^{1/2}-(2\varepsilon+1)^{1/2}-\ln\frac{(2\varepsilon z^2)^{1/2}+(2\varepsilon z^2+1)^{1/2}}{(2\varepsilon)^{1/2}+(2\varepsilon+1)^{1/2}}\right] \qquad (19)$$

where $z \equiv r_s/r_b$. For planar bodies ($j = 0$) we obtain

$$x = \frac{4r_b^{3/2}}{3K_1\varepsilon^{3/2}}\left[(\varepsilon z-1)(2\varepsilon z+1)^{1/2}-(\varepsilon-1)(2\varepsilon+1)^{1/2}\right] \qquad (20)$$

For large z, these results take the same form as given by blast-wave theory. Near the nose, however, the finite thickness of the body is taken into account.

A comparison of Eq. (20) with the flat-plate data of Cheng et al.[8] is shown in Fig. 1, with $d = 2r_b$. The over-all agreement between experiment and theory is very good. The worst agreement is near the nose as might be expected. Both the data and theory show significant deviation from the straight-line behavior characteristic of first-order blast-wave results on log-log plots. A number of other comparisons are discussed in Ref. 1.

References

[1] Fiorino, T. D., "An Integral Approximation for Shock Shapes over Slender Bodies in Inviscid Hypersonic Flow," Ph.D. thesis, 1970, Dept. of Aerospace and Mechanical Engineering, University of Oklahoma, Norman, Okla.

[2] Chernyi, G. G., *Introduction of Hypersonic Flow*, 1st ed., Academic Press, New York, 1961, Chap. 5.

[3] Rasmussen, M. L., "On Hypersonic Flow Past an Unyawed Cone," *AIAA Journal*, Vol. 5, No. 8, Aug., 1967, pp. 1495–1497.

[4] Linnell, R. D., "Two-Dimensional Airfoils in Hypersonic Flows," *Journal of Aerospace Sciences*, Vol. 16, 1949, pp. 22–30.

[5] Van Dyke, M. D., "A Study of Hypersonic Small Disturbance Theory," Rept. 1194, 1954, NACA.

[6] Yakura, J. K., "Theory of Entropy Layers and Nose Bluntness in Hypersonic Flow," *Hypersonic Flow Research*, Vol. 7, edited by F. R. Riddell, Academic Press, New York, 1962, pp. 421–470.

[7] Guiraud, J. P., Vallee, D., and Zolver, R., "Bluntness Effects in Hypersonic Small Disturbance Theory," *Basic Developments in Fluid Dynamics*, Vol. 1, edited by M. Holt, Academic Press, New York, 1965.

[8] Cheng, H. K., Hall, J. G., Golian, T. C., and Hertzberg, A., "Boundary-Layer Displacement and Leading-Edge Bluntness Effects in High Temperature Hypersonic Flow," *Journal of Aerospace Sciences*, Vol. 28, No. 5, 1961, pp. 353–381, 410.

Stability of a Spinning Satellite with Flexible Antennas

W. N. Dong*

Memorial University of Newfoundland, St. John's, Newfoundland, Canada

AND

A. L. Schlack Jr.†

University of Wisconsin, Madison, Wisc.

Nomenclature

A, B, C	= principal moments of inertia of the rigid body about the x, y, z body axes, respectively
a_{ij}	= coefficients of quadratic terms in total kinetic energy expression
E	= Young's modulus
h	= distance from clamped end of beam to 0
I_x, I_y, I	= area moments of inertia of the elastic beam
l	= length of beam
M_t	= total system mass
0	= mass center of the complete system at dynamic equilibrium
p_k	= generalized momenta
q_k	= generalized coordinates
R_A	= ratio of mass moment of inertia of the pair of antennas about the x axis to A
T	= kinetic energy
T_R	= rotational kinetic energy
u_x, u_y	= displacement of a beam element relative to the rigid body
U	= dynamic potential
V	= potential energy of the system
v_c	= velocity of the system's mass center
x, y, z	= body axes coordinates
x_1, y_1, z_1	= body axes coordinates at dynamic equilibrium state
ψ, ϕ, θ	= Euler angles
ρ	= mass per unit length of elastic beam
π_1	$= \rho l/M_t$
π_2^2	$= EI/(\rho l^4)$
π_3	$= \rho l^3/A$
π_4	$= h/l$
π_5	$= \rho h^3/A$
$\bar{\pi}_3$	$= \rho l^3/B$
$\bar{\pi}_5$	$= \rho h^3/B$

Introduction

THE dynamic stability of spinning satellite systems with elastic components is an important space dynamics problem which has been receiving much attention in the recent literature. Because of the inherent analytical difficulties involved in studying such hybrid dynamical systems, many approximate techniques have evolved in the literature. The dynamic stability of flexible satellite systems has been studied by a wide variety of methods for several different configurations, with Liapunov's direct method being one of the more widely used techniques.

Recent papers by Meirovitch and Calico[1] and Barbera and Likens[2] present interesting discussions and comparisons between the various analytical methods available in the literature, which would make a further historical development redundant at this point. Of particular interest here is the use of Liapunov's direct method applied to elastic spacecraft, a subject which has been discussed by many researchers too numerous to mention. However, papers by Pringle,[3] Meirovitch,[4–6] Barbera and Likens,[2] Hughes and Fung,[7] Brown and Schlack,[8] and Kulla[9] are considered representative of these studies.

Received October 26, 1973; revision received July 1, 1974.

Index categories: Spacecraft Attitude Dynamics and Control; Structural Dynamic Analysis.

* Postdoctoral Fellow; formerly Graduate Student, University of Wisconsin, Madison, Wisc.

† Professor of Engineering Mechanics. Member AIAA.